

<https://doi.org/10.18524/1810-4215.2023.36.290189>

ANGULAR STRUCTURE OF THE RADIO GALAXY 3C280 AT DECAMETER WAVELENGTHS

R.V. Vashchishyn¹, V.A. Shepelev², O.A. Litvinenko³, G.S.Podgorny², A.V. Lozinsky⁴

¹ Gravimetric Observatory of IGP NASU, Poltava, Ukraine, vrv.uran2@gmail.com

² Institute of Radio Astronomy of NASU, Kharkiv, Ukraine, vshep258@gmail.com

³ URAN-4 Laboratory of IRA NASU, Odesa, Ukraine

⁴ Physical and Mechanical Institute of NASU, Lviv, Ukraine

ABSTRACT. The image of the 3C280 radio galaxy at decimeter wavelengths consists of two emission regions, the centers of which are separated by about 13 arc seconds. These regions are lobes of the radio galaxy with bright compact components or hot spots embedded in them. We present the results of a study of the source structure in the decameter wavelength range, carried out with the URAN-1 – URAN-4 radio interferometers using a especially technique developed. We show, that at the decameter wavelengths, the source model contains two extended components with the size and position as the lobes have in the decimeter range and a compact detail corresponding to one of the hot spots. The radio emission of other hot spots is not detected at the decameter waves due to their low flux density. The spectra of the radio galaxy components and their variation in the range from decameter to decimeter wavelengths are determined in this study. It is found, that extended lobes provide about 70% of 3C280 flux at low frequencies in contrast to the high-frequency image of the radio galaxy, where compact hot spots predominate in the source radiation.

Keywords: radio source, interferometer, decameter range, brightness distribution, decameter model.

АНОТАЦІЯ. Зображення радіогалактики 3C280 на дециметрових довжинах хвиль складається з двох областей випромінювання, центри яких рознесені приблизно на 13 кутових секунд. Ці області є пелюстками радіогалактики з яскравими компактними компонентами або вбудованими в них гарячими плямами. Наведено результати дослідження структури джерела в декаметровому діапазоні довжин хвиль, що були виконані на радіоінтерферометрах УРАН-1 – УРАН-4 за спеціально розробленою методикою. Ми показуємо, що на декаметрових хвилях модель джерела містить два протяжних компонента з розміром і положенням пелюсток, як у дециметровому діапазоні та компактну деталь, що відповідає одній із гарячих плям. Радіовипромінювання інших гарячих плям на декаметрових хвилях не реєструється через їх малу густину потоку. У цьому дослідженні визначено спектри компонентів радіогалактики та їх зміну в діапазоні від декаметрових

до дециметрових довжин хвиль. Виявлено, що протяжні пелюстки забезпечують близько 70% потоку 3C280 на низьких частотах, на відміну від височастотного зображення радіогалактики, де компактні гарячі плями переважають у випромінюванні джерела.

Ключові слова: радіоджерело, інтерферометр, декаметровий діапазон, розподіл яскравості, декаметрова модель.

1. Introduction

Radiogalaxy 3C280 is a compact FR II radio source with a steep spectrum. It is located in a distant galaxy cluster and has a redshift of $z=0.996$. A massive elliptical galaxy identified with this radio source is located at its center. (Zirm, 2003). Quite powerful, with an interesting morphology, 3C280 attracted our attention with its complex angular structure at high frequencies (Allen et al., 1972; Clark et al., 1966; Wraith, 1972; Wilkinson, 1972; Mullin et al., 2006; Laing, 1981; Bovkun et al., 1981; Readhead et al., 1976) and the almost complete absence of data about it in the decameter range. In this work, we want to conduct investigations of this source at the lowest frequencies, not limited by the transparency of the ionosphere, and obtain the angular brightness distribution. We also want to find out what possible changes in its structure may occur and determine their probable causes.

From numerous radio images of 3C280 obtained at different times, for analysis and comparison, we chose maps obtained with MERLIN interferometers and the VLA synthesis system (Mullin et al., 2006).

On the map obtained at the VLA at a frequency of 1.4 GHz (Xu et al., 1995) with a resolution of 1.5" (see Fig. 2), extended regions of diffuse synchrotron radiation – lobes – are clearly visible. They are located symmetrically to the east and west relative to the center of the source, which contains the galactic nucleus (due to low flux at these frequencies, it is not visible). The eastern lobe is about 3", and the western lobe is about 4". Hot spots on this map, due to its low resolution, are not completely resolved. In the eastern lobe, the hot spot has a radial shape and is located in the

center of the lobe; in the western one, it is slightly elongated in the northwest direction and lies closer to the edge.

On the contrary, no lobes are observed on the maps from (Mullin et al., 2006), which have a resolution of 0.35" and 0.06". However, hot spots are clearly visible. Several compact brightness regions are visible in place of the elongated hot spot on the map at 1.5" resolution.

So, having at our hands a system of decameter radio interferometers URAN and a map obtained at VLA at 1.4 GHz (Xu et al., 1995), which have approximately the same resolution, we decided to compare the brightness distribution of 3C280 at high and low frequencies.

2. Observations and data processing

Observations of 3C280 were carried out using the Ukrainian decameter VLBI network URAN (Megn et al., 1997) simultaneously at frequencies of 20 and 25 MHz. Interference oscillations were formed by multiplying the signals from the north-south antenna of the UTR-2 radio telescope with the signals from the antennas of the URAN system. The measurements were carried out in separate sessions in the autumn-winter period for several days at hourly angles of ± 240 minutes relative to the culmination. The data obtained at each hourly angle were averaged for all observation days, and then the weighted average value of the visibility module and its error were calculated. An example of the experimental values obtained and their errors for the URAN-1 and URAN-2 interferometers are shown in Fig. 1 by symbols 1 and 3.

As is known, the inverse Fourier transform of a similar set of values obtained on different bases represents the source brightness distribution. For this, the necessary conditions are the availability of information about the phase, good filling of the spatial frequency plane, and a sufficient signal-to-noise ratio. However, at decameter waves, wavefront distortions due to the influence of ionospheric irregularities on the propagation of radio waves lead to a phase shift of the measured visibility between antennas more than 2π radians. Also, the signal-to-noise ratio at large bases can be about 1, and the coverage of the uv -plane in our observations is not sufficient. All this makes it impossible to use this method of image restoration, therefore to determine the

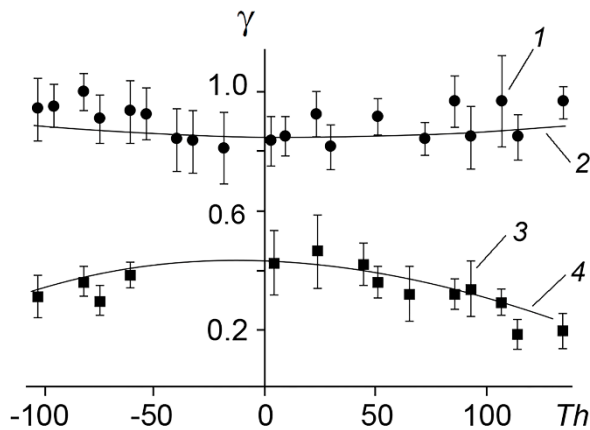


Figure 1: Visibility modulus at a frequency of 25 MHz: 1, 2 – experimental and calculated for URAN-1; 3, 4 – experimental and calculated for URAN-2

radio brightness distribution of sources in the decameter range, we use a model selection method without information about the phase of the visibility function.

Quite well known, this method has proven its effectiveness in many of our investigations we have conducted. It is described in (Megn et al., 2001) and consists of representing the real source brightness distribution in the form of a model consisting of a certain number of elliptical components with arbitrary axes orientation and a Gaussian radio brightness distribution.

The process of obtaining a model consists of a sequential step-by-step change of the initial parameters (dimensions, fluxes, coordinates, inclination, etc.) and repeated calculations of the interferometer response. This operation aims to minimize the sum of the least squares of deviations between the calculated response and the experimental one. In this way, the resulting model is consistent with the experimental dependences of the visibility modulus on the hour angle for all bases and frequencies.

To facilitate the calculation of the decameter model, its correctness, and accuracy, we use a priori information from the literature to find the parameters of the initial approximation. We take such information from digital maps of the source, obtained at frequencies as close as possible to ours, and with an angular resolution no worse than that of the URAN-3 radio interferometer, which has the largest base of about 900 km. From the selected map, we calculate the dependence of the visibility modulus on the hour angle for interferometers with our geometry. Next, we select a simple model using the least squares method. The interferometer responses from this model and from the map should be as close as possible.

In our case, to determine the initial parameters for the search of a decameter model, we used the 3C280 digital map, obtained at VLA at a frequency of 1.4 GHz with a resolution of 1.5" (Xu et al., 1995). The model calculated from this map is presented in Fig. 2, and its parameters are summarized in Table 1.

Fitting the model to the digital map made it possible to identify the structural components of the high-frequency image – two lobes and two hot spots: one in the western lobe and one in the eastern. At the same time, in the western lobe the hot spot has a small visible extent (see Fig. 2). On

Table 1: Model from the 1.4 GHz map

| Detail | α , " | δ , " | S/S_0 | θ , " | a/b | ψ , ° |
|-------------------|--------------|--------------|---------|------------------|-------|------------|
| HS _E | 6,34 | 0 | 0,19 | 1,5 | 1 | 0 |
| BCA1 | -6,34 | 0 | 0,29 | 1,2 | 1 | 0 |
| BCA2 | -6,02 | 0,5 | 0,32 | 2,9x2,0 (2,4) | 1,41 | -50 |
| Lobe _E | 6,34 | 0 | 0,07 | 2,4 | 1 | 0 |
| Lobe _W | -3,9 | 0,8 | 0,13 | 5,3x3,3 (4,2) | 1,6 | 72 |

Notes: α , δ – coordinates of the components relative to the conventional geometric center of the source; S/S_0 – share in the total flux; θ – size; a/b – ellipticity; ψ – position angle; BCA1,2 – bright compact regions in the western lobe.

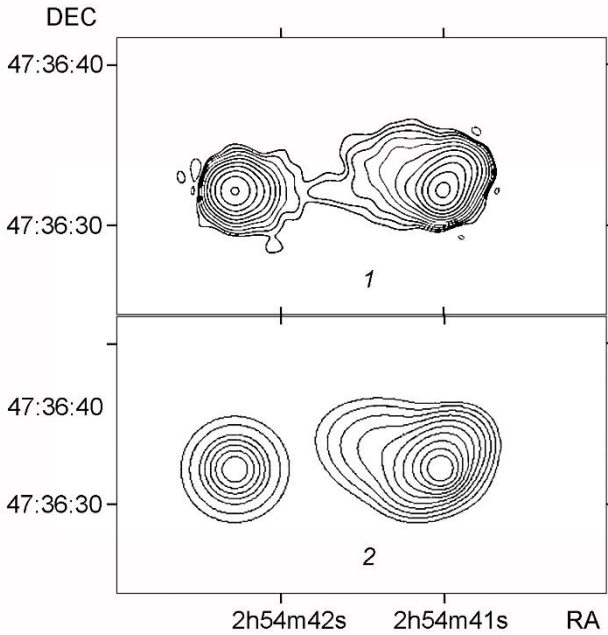


Figure 2: Radio galaxy 3C280 at 1.4 GHz: 1 – map from (Xu et al., 1995); 2 – model

the ultra-high-resolution map from (Mullin et al., 2006), as discussed above, in place of the elongated hot spot, several compact brightness regions are there. To better match the interferometric response, we modeled it as two nearby compact bright regions.

3. Results

Comparison of the visibility modulus experimental dependences on the hour angle with the ones fitted to the high-frequency map for all decameter interferometers made it possible to identify their differences. They occur due to changes in the spectral characteristics of the source components at low frequencies. Thus, for URAN-2 the experimental visibility is about 40% instead of the calculated 75%; on URAN-4 it is 25% instead of the calculated 45%; the response from the URAN-3 interferometer turned out to be below 8% instead of the calculated 17% at the maximum of fluctuations. All these changes are due to an increase in the share of the flux of extended components, and an increase in the size of compact components, including the scattering. The experimental response from the URAN-1 interferometer is quantitatively equal to the calculated one since the image of the radio galaxy does not contain large formations ($>20''$) with low surface brightness. Therefore, URAN-1 sees all detected components in 3C280 as point sources and does not resolve them.

To search the decameter model, we extrapolated the resulting high-frequency model to low frequencies, taking into account all our knowledge about the spectral characteristics of the components and the scattering angle of radio emission in the interstellar medium. Next, we selected the flux ratios of the components, then their ellipticity and inclination. In this model (see Table 2), the sizes of the components, compared with those given in Table 1, changed by the value of the scattering angle. In our case, according to (Shyshov, 2001), at 25 MHz it is $0.9''$, and at 20 MHz it is

Table 2: Decameter model of 3C280

| Detail | α'' | δ'' | S/S_0 | θ_{25}'' | θ_{20}'' | a/b | ψ° |
|-------------------|------------|------------|---------|-----------------|-----------------|-------|--------------|
| HS _w | -6,34 | 0 | 0,3 | 1,7 | 2,1 | 1 | 0 |
| Lobe _E | 5,6 | 0 | 0,3 | 2,5 | 2,9 | 1 | 0 |
| Lobe _w | -3,9 | 0,8 | 0,4 | 4,3 | 4,6 | 1,6 | 72 |

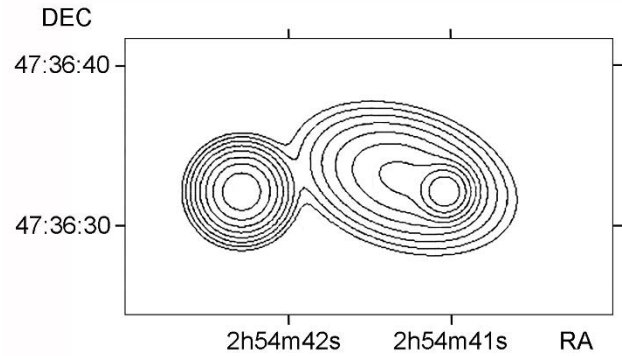


Figure 3: Model 3C280 obtained at 25 MHz

$1.47''$. Two bright compact regions in the western lobe, which simulated an elongated hot spot at high frequencies, are observed as one. On high-resolution maps (Mullin et al., 2006), the position of this region in the group of spots corresponds to a hot spot with the highest brightness and small size. The coordinates of the hot spots have not changed; the eastern lobe has shifted slightly towards the center.

Comparing the fluxes of components of high-frequency and decameter images given in Table 1 and Table 2, it should be noted that in the decameter range, about 70% of the flux density is formed by extended elements – lobes. Their radiation, compared to hot spots, has a steeper spectrum. The western hot spot accounts for 30%. Our data are consistent with the size and flux of the scintillating component at 25 MHz obtained in (Bovkun, 1981). Since radiation from the eastern hot spot is not observed at low frequencies, we can say with confidence that in (Bovkun, 1981) and (Readhead, 1976) the scintillating component is the western hot spot. At high frequencies, about 80% of the radiation is formed by hot spots.

For example, in Fig. 1 solid curves 2 and 4 show the calculated hourly dependencies of the decameter model for the URAN-1 and URAN-2 interferometers, in Fig. 3 – model that we obtained at 25 MHz. Here the radio image is presented in isophotes on a logarithmic scale. Systematic errors do not exceed 15%.

Fig. 4 shows the spectral characteristics of 3C280. The data obtained in this work is shown at frequencies of 20 and 25 MHz.

The full spectrum of the source was fitted by linear approximation of literature data (Vigotti et al., 1999; Roger et al., 1986; Kuehr et al., 1981; Herbig et al., 1992) using the least mean squares method from 10 to 5000 MHz. In the region from 20 to 1000 MHz, it is linear and does not have any curvatures caused by various known mechanisms (Herbig et al., 1992).

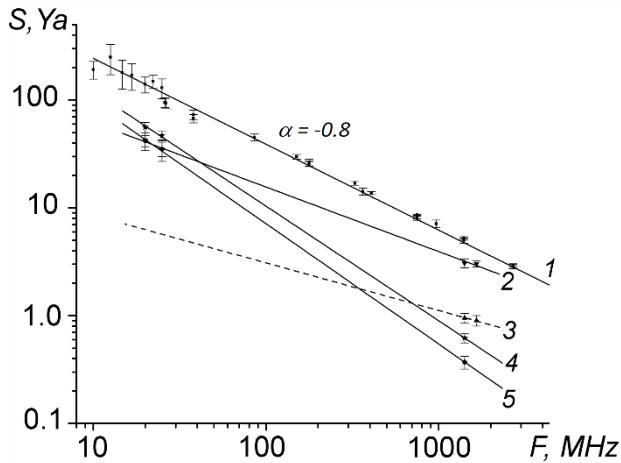


Figure 4: The spectrum of 3C280 and the probable spectra of its components: 1 – total spectrum of the source; 2, 3 – western and eastern hot spots; 4, 5 – western and eastern lobes

Since we do not have information about any curvature of the spectra of extended components, we assume them linear in this range. They were approximated from data taken from digital maps obtained at frequencies of 1.658 GHz on MERLIN ("MERLIN/e-MERLIN is a National Facility operated by the University of Manchester at Jodrell Bank Observatory on behalf of STFC, part of UK Research and Innovation") and 1.4 GHz on VLA (Xu et al., 1995), as well as taking into account our data at 20 and 25 MHz.

As can be seen from the figure, the change in the image from high to low frequencies is determined by the spectra of the components. At decimeter and especially centimeter waves, hot spots have the greatest brightness. Extended details, and lobes, are practically not observed. With increasing the length of the wave the redistribution of fluxes occurs: extended regions emit long waves more intensely, while compact regions become noticeably weaker due to the lower values of their spectral indices. Thus, the emission intensity of the eastern hot spot at decimeter waves turned out to be insufficient for stable detection by our instrument.

4. Conclusion

For the first time, the angular structure of the radio galaxy 3C280 was studied using the interferometric method in the decimeter wavelength range. Models of the brightness distribution at frequencies of 20 and 25 MHz were obtained, and the probable spectral characteristics of the radio source were determined. It was found that:

1) The sizes of extended components did not change with decreasing frequency. In place of the group of compact bright regions, which at 1.4 GHz formed a slight elongation of the western hot spot, only one remained, the brightest, with a flux fraction of 30%. Its size is determined by scattering on the interstellar medium;

2) About 70% of the total flux at low frequencies is formed by extended components - lobes, while at high frequencies 80% of the radiation is provided by hot spots. The size and contribution of the compact component to the flux of decimeter radiation are consistent with the results of studies of 3C280 previously conducted at 25 MHz by the scintillation method on inhomogeneities of the interplanetary plasma;

3) The eastern hot spot flux lies below the sensitivity threshold of our instrument and does not affect the interferometric response.

Acknowledgements. V.A. Shepelev acknowledges the Europlanet 2024 RI project funded by the European Union's Horizon 2020 Research and Innovation Programme (Grant agreement No. 871149).

The authors express their gratitude to David Williams from the Jodrell Bank Observatory for providing the necessary materials for this work.

References

- Allen, L.R., Anderson, B., Conway R.G. et al.: 1972, *Mon. Not. R. Astron. Soc.*, **124**, 477.
 Bovkun, V. P., Zhuk, I. N., Men, A. V.: 1981, *Soviet Astronomy Letters*, **7**, 192.
 Clark B.G., Hogg D.E.: 1966, *Astrophys. J.*, **145**, 210.
 Herbig T., Readhead A. C. S.: 1992, *Astron. Astrophys. Suppl. Ser.*, **81**, 83.
 Kuehr H., Witzel A., Pauliny-Toth I. I. K. et al.: 1981, *Astron. Astrophys. Suppl. Ser.*, **45**, 367.
 Laing R. A.: 1981, *Mon. Not. R. Astron. Soc.*, **195**, 261.
 Megn A.V., Braude S.Ya., Rashkovsky S.L., et al.: 1997, *Radio phys. radio astron.*, **2**, 4, 385.
 Megn A.V., Rashkovsky S.L., Shepelev V.A.: 2001, *Radio phys. radio astron.*, **6**, 1, 9.
 Mullin L. M., Hardcastle M. J., Riley J. M.: 2006, *Mon. Not. R. Astron. Soc.*, **372**, 113.
 Readhead, A. C. S., Hewish, A.: 1976, *Mon. Not. R. Astron. Soc.*, **176**, 571.
 Roger, R. S., Costain, C. H., Stewart, D. I.: 1986, *Astron. Astrophys. Suppl. Ser.*, **65**, 485.
 Shyshov V.I.: 2001, *Astron. J.*, **78**, 3, 229.
 Vigotti M., Gregorini L., Klein U. et al.: 1999, *Astron. Astrophys. Suppl. Ser.* **139**, 359.
 Wilkinson P. N.: 1972, *Mon. Not. R. Astron. Soc.*, **160**, 305.
 Wraith P. K.: 1972, *Mon. Not. R. Astron. Soc.*, **160**, 283.
 Xu W., Readhead A. C. S., Pearson, T. J. et al.: 1995, *Astrophys. J. Suppl. Ser.*, **99**, 297.
 Zirm W.: 2003, *Astrophys J*, 585, 90.